

Static stress demagnetization of single and multidomain magnetite with implications for meteorite impacts

STUART A. GILDER*†‡, MAXIME LE GOFF† and JEAN-CLAUDE CHERVIN§

†Institut de Physique du Globe de Paris, Equipe de Paléomagnétisme, 4 place Jussieu,
75252 Paris Cedex 05, France

‡Department of Earth and Environmental Sciences, Geophysics Section, Ludwig Maximilians
University, Theresienstrasse 41, 80333 Munich, Germany

§Département de Physique des Milieux Denses, Institut de Minéralogie et de Physique des Milieux
Condensés, Université Pierre et Marie Curie, CNRS-UMR 7590, 140 rue de Lourmel,
75015 Paris, France

(Received 3 July 2006; revised 25 August 2006; in final form 22 September 2006)

Stress demagnetization effects on ferromagnetic minerals are poorly known, especially above 1 GPa, and when initially magnetized under pressure and then subjected to further stress. Our experiments on pure magnetite under quasi-hydrostatic loads in the presence of a small (Earth's) field show that stress demagnetization depends on domain state and stress history. Viewed globally, the results follow a simple law where the percentage loss in magnetic moment is the inverse of pressure (*e.g.*, 50% loss in moment at 1 GPa, 67% loss at 2 GPa, etc.). Our experiments also quantify the effect of demagnetization upon stress release, where the moment upon full decompression is two-thirds less than the moment when decompression first began. Given the magnitude of the stress demagnetization effect, we conclude that the presence or absence of a planetary magnetic field cannot be deduced from the magnetic fields measured over meteorite craters, such as those on Mars.

Keywords: Stress; Demagnetization; Magnetite; Meteorite crater

1. Introduction

With the advent of paleomagnetic studies in the 1940s, scientists began to wonder how the effect of stress, from burial, folding, etc., would influence the magnetic remanence of rocks. By the mid 1950s, an intense research effort was underway aimed at understanding piezo-remanence, which is the remanent magnetization produced by stress, as well as the opposite effect of stress demagnetization. Laboratory experiments suggested that the magnetic signals of rocks were sensitive to stresses typically found around fault zones [1–5]. And it was calculated

*Corresponding author. Tel.: +33-144274934; Email: gilder@ipgp.jussieu.fr and gilder@geophysik.uni-muenchen.de

that such stress-induced changes would in turn modify the local magnetic field [6–9]. Scientists thought that by monitoring magnetic field variations, earthquakes or volcanic eruptions could be predicted [10]. However, field observations of a pressure-induced magnetic effect proved elusive. More convincing evidence for stress-induced magnetization changes in nature comes from meteorite impact craters, which are often characterized by lower than average magnetic anomalies. For example, magnetic surveys of the Martian surface detect significantly lower magnetic field intensities over the gigantic impact craters Hellas and Argyre than over the surrounding regions [11–13]. The reduced fields are commonly attributed to pressure demagnetization caused by shock waves generated during meteorite impact in the absence of a planetary field [13–15].

The effect of stress in the absence of an external magnetic field has a permanent demagnetizing effect on rocks that contain an assemblage of magnetic grains. In this case, permanent means that once the pressure is released, the magnetic moment does not grow back to its original (pre-compressed) value because the magnetic vector directions of the grains have been randomized, thus lowering the net magnetization of the rock. It does not mean that the individual magnetic grains have lost their capacity to be magnets. This makes stress demagnetization similar in theory to alternating field demagnetization [16]. However, quantifying stress demagnetization is difficult because the magnetization of the pressure vessel must be significantly lower than that of the sample, and the cell must not interfere with the electronics of the detector. In order to amplify the magnetic signal, one needs to maximize the number of magnetic grains, which explains why most experimental work on this problem has focused on large rock samples. Because a trade-off exists between pressure and sample size, most experiments have been performed using uniaxial stresses, at pressures lower than 1 GPa (10 kbar), with most measurements taking place after pressure release.

Despite the experimental restrictions, several aspects of stress demagnetization are known. Martin and Noel [17] demonstrated the differences between hydrostatic and uniaxial stress demagnetization on a diabase rock containing large (20–300 micron) titanomagnetite (Curie temperature = 535 °C) grains. Their experiments showed that uniaxial stresses demagnetize this material about two times more than hydrostatic stresses; *e.g.*, at 100 MPa, hydrostatic and uniaxial pressures demagnetize roughly 20% and 40% of the original, non-compressed magnetization intensity, respectively. Adding a shear component to a static uniaxial stress will demagnetize rocks even faster [18]. Another observation from high-pressure experiments performed under uniaxial stress is that magnetic properties change in relation to the maximum stress axis direction [19–22]. For stress demagnetization, the magnetization intensity decreases faster parallel to the maximum stress direction rather than perpendicular to it; magnetic susceptibility increases perpendicular to the maximum stress direction and decreases parallel to it. Kletetschka *et al.* [23] shocked a variety of magnetic mineral aggregates to pressures around 1 GPa. They found a correlation between the percentage of retained magnetization and magnetic coercivity, consistent with previous work [*e.g.*, 24–27]. Gattacceca *et al.* [28] combined pulsed laser shocks with magnetic microscopy on natural titanomagnetite-bearing basalt. They found that 1 GPa pressures remove 70–80% of the initial magnetization.

To our knowledge, previous investigations have largely ignored how grain size, composition, etc. bear on stress demagnetization while the sample is under pressure. Moreover, decompression effects have not been quantified. For these reasons, we developed new high-pressure cells that facilitate direct measurements of the full magnetic vector to pressures of ~40 GPa, which allows one to experiment on magnetic minerals whose composition and grain sizes are well characterized.

2. Experimental procedure and results

We designed a Merrill–Basset-type diamond anvil cell made solely of BeCu, including the aligning screws. Fe-pure (Ti-free) single and multidomain magnetite, previously described in Gilder *et al.* [29, 30], were loaded together with ruby spheres and silica gel in a cylindrical chamber drilled in a bronze-Be gasket with a diameter and height (after work hardening) of 400 μm and 100 μm , respectively. Silica gel served as a pressure medium to maintain hydrostatic pressures, as attested to by well-defined $R1$ and $R2$ peaks in the ruby fluorescence spectra [31]. Stresses were not perfectly hydrostatic, as a 10% difference in pressure exists between rubies in the center of the cell versus those near the edge. The grains easily disaggregate after depressurizing from 5 GPa; they are not compacted into a solid mass. After loading, a direct current (dc) field of 315 mT was applied parallel to the plane of the diamond cutlets so that the samples would acquire an isothermal remanent magnetization (IRM). The magnetic remanence of the sample was measured by inserting the cell directly into a 2G Inc. three-axis cryogenic magnetometer. Pressure was then raised or lowered sequentially in the Earth’s magnetic field in Paris ($\sim 48,000$ nT) at room temperature, with the magnetic remanence being measured at each pressure step. We also applied a 315 mT field to the samples while they were under pressure to observe the stress demagnetization effect on a sample whose magnetization was acquired under stress. The cell itself acquires a slight magnetic remanence from the applied field, which remains constant throughout an experiment, that was subtracted from the total measured moment.

Figure 1 shows the pressure path and corresponding magnetic moments of the experiments performed on the same multidomain magnetite sample (data in table 1). Starting from ambient pressure ($P = 0$ GPa), the magnetization decreased to 21% of the original value by 2.03 GPa. After a new 315 mT field was imposed at 2.03 GPa, the moment decreased faster with increasing pressure than when starting from ambient conditions. This suggests that a multidomain

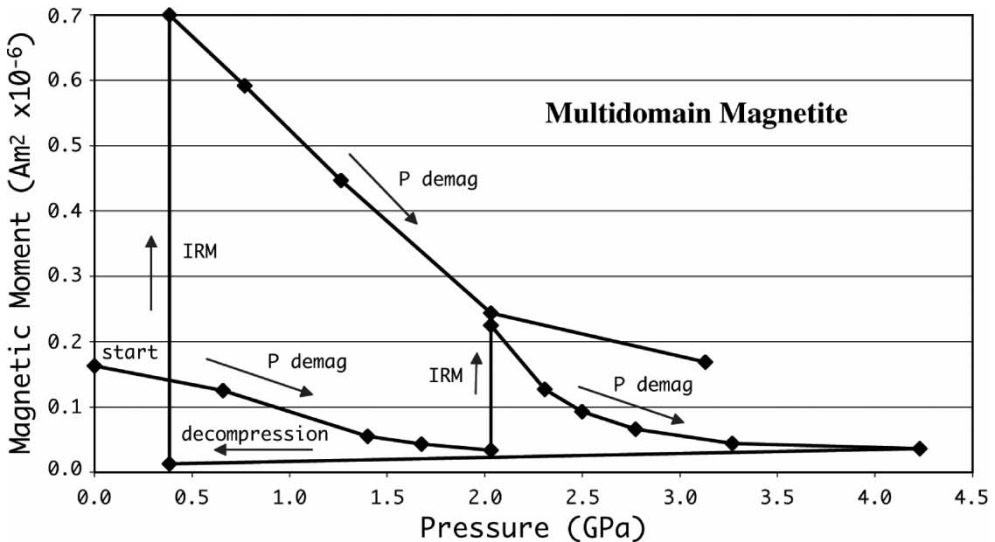


Figure 1. Stress demagnetization of multidomain magnetite. A direct field of 315 mT was applied to the sample at ambient conditions to create an isothermal remanent magnetization (IRM) ('start' in figure). The magnetic remanence was then measured under pressure at successively higher pressures until 2.03 GPa, then a new 315 mT field was applied to the sample, which was then compressed to successively higher pressures until 4.23 GPa. Pressure was then released, a new 315 mT field imposed, followed by a third round of stress demagnetization.

Table 1. Stress demagnetization data.

Single domain magnetite			Multidomain magnetite		
Pressure (GPa)	M ($\text{Am}^2 \times 10^{-6}$)	M norm	Pressure (GPa)	M ($\text{Am}^2 \times 10^{-6}$)	M norm
IRM – 1st compression			IRM – 1st compression		
0.16	0.365	1.00	0.00	0.163	1.00
0.38	0.216	0.59	0.66	0.125	0.77
0.82	0.150	0.41	1.40	0.055	0.34
1.07	0.119	0.33	1.68	0.043	0.26
1.57	0.089	0.24	2.03	0.034	0.21
1.81	0.054	0.15			
IRM – 2nd compression			IRM – 2nd compression then decompression		
1.81	1.132	1.00	2.03	0.225	1.00
1.92	1.062	0.94	2.31	0.127	0.56
2.11	0.952	0.84	2.50	0.093	0.41
1st decompression			2.77	0.066	0.29
2.11	0.952	1.00	3.27	0.044	0.20
1.48	0.861	0.90	4.23	0.036	0.16
1.02	0.742	0.78	0.38	0.013	0.06
0.60	0.412	0.43			
0.16	0.315	0.33			
IRM – 3rd compression			IRM – 3rd compression		
0.16	0.800	1.00	0.38	0.700	1.00
0.85	0.672	0.84	0.77	0.592	0.85
1.29	0.571	0.71	1.26	0.447	0.64
1.95	0.509	0.64	2.03	0.244	0.35
2.22	0.491	0.61	3.13	0.169	0.24
IRM – 2nd decompression					
2.22	1.212	1.00			
1.57	1.112	0.92			
1.21	0.942	0.78			
0.93	0.766	0.63			
0.55	0.476	0.39			
0.11	0.395	0.33			

Abbreviations: M: magnetic moment; M norm: magnetic moment normalized by the maximum value in a given run; IRM: isothermal remanent magnetization. Non-normalized data are shown in figures 1 and 2.

magnetite-bearing rock that acquired its moment at depth, and was subsequently compressed, demagnetizes faster than an equivalent rock that formed near the surface and was then compressed. Although the decompression effect on the moment appears negligible in figure 1, the moment actually decreases nearly three times from 4.23 GPa to 0.38 GPa. Upon a new round of compression, the moment decreased, but slower than during the first compression run (figure 1).

Figure 2 shows the pressure path and corresponding magnetic moments of the experiments performed on the same single domain magnetite sample (data in table 1). We paid close attention to the effects of decompression in these experiments. Starting from ambient pressure, the magnetization decreased to 15% of the original value by 1.81 GPa. After a new 315 mT field was applied at 1.81 GPa, the IRM moment decreased slower with increasing pressure than when starting from ambient conditions. This suggests that a single domain magnetite-bearing rock that acquired its remanence at depth and was then compressed demagnetizes slower than an equivalent rock formed at the surface and was then compressed. The sample was then stepwise decompressed to 0.16 GPa, a 315 mT field was imparted, followed by a third round of compression up to 2.22 GPa. Another 315 mT field was applied at 2.22 GPa, then the pressure was incrementally decreased.

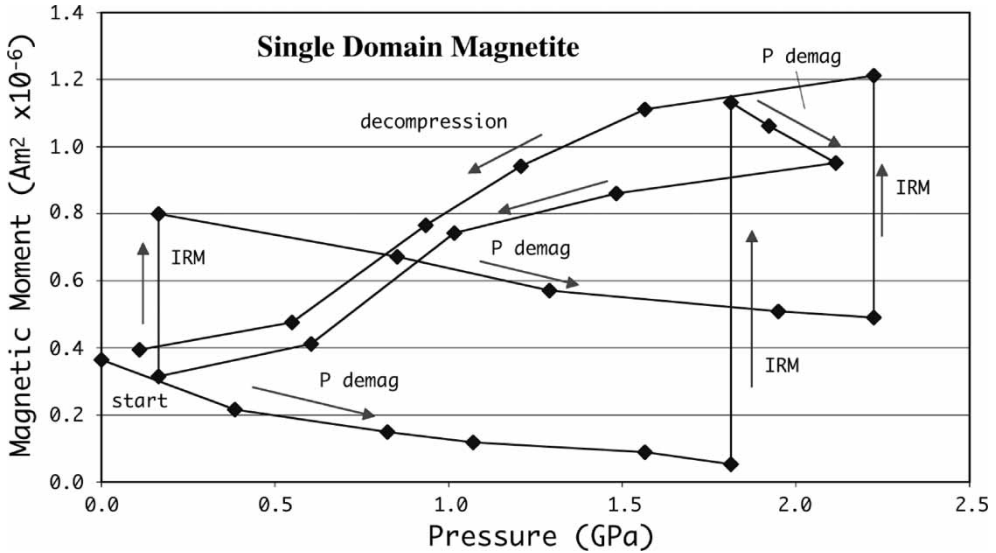


Figure 2. Stress demagnetization of single domain magnetite. A direct field of 315 mT was applied to the sample at ambient conditions to create an isothermal remanent magnetization (IRM) ('start' in figure). The magnetic remanence was then measured under pressure at successively higher-pressures until 1.81 GPa, then a new 315 mT field was applied to the sample. This newly acquired IRM moment was then measured under pressure at successively higher-pressures until 2.11 GPa, and then pressure was sequentially released. A new 315 mT field was imposed, followed by a new round of stress demagnetization until 2.22 GPa, where another 315 mT field was applied, and then the cell was sequentially decompressed.

We normalized the magnetic moment during a given compression or decompression run to the moment measured at the start of the run (the IRM moment in most cases) (figures 3 and 4). For the compression runs (figure 3), pressure is displayed relative to the initial pressure at the beginning of the run, called delta pressure (ΔP), which is the pressure at step n (P_n) minus the initial pressure (P_i) when the particular run began ($\Delta P = P_n - P_i$). For decompression (figure 4), pressure is normalized relative to the pressure when decompression began (P_n/P_i). Qualitatively, for the first compression cycle (figure 3), which might correspond to a rock that crystallized near the surface and was then compressed, one sees that multidomain magnetite demagnetizes less easily than single domain magnetite. For magnetite that cooled through its Curie point while under pressure, such as a rock lying at considerable depth in a slowly cooling planet, the opposite is true, single domain magnetite better resists pressure demagnetization than multidomain magnetite. Finally, for work-hardened minerals, *e.g.*, those subjected to multiple stress cycles, such as a rock bombarded by successive impacts yet somehow remagnetized after the last impact, both single and multidomain magnetite increase their resistance to pressure demagnetization.

The results follow fairly simple quantitative rules. Previously uncompressed single domain magnetite or multidomain magnetite formed at depth will lose their magnetizations roughly as $M_{P_n}/M_{P_i} = 1/P_n^2$ (or approximately exponentially $M_{P_n}/M_{P_i} = e^{-P_n}$), where $(M_{P_n}/M_{P_i}) \times 100$ is the percentage of the initial moment (M_{P_i}) remaining at P_n , which is the pressure, in GPa, above the initial pressure, P_i (where P_i is treated in the same way as in figure 3). Previously unstrained multidomain magnetite or single domain magnetite-bearing rocks formed at depth will lose their remanences roughly following a linear law valid below 1.5 GPa where $M_{P_n}/M_{P_i} \approx -0.45P_n + 1$. In the case of large meteorite impacts where pressure waves penetrate deeply (several 10s of kilometers), one could use a general rule of $1/P$ for the decrease in the percentage of original magnetization for the entire volume of affected

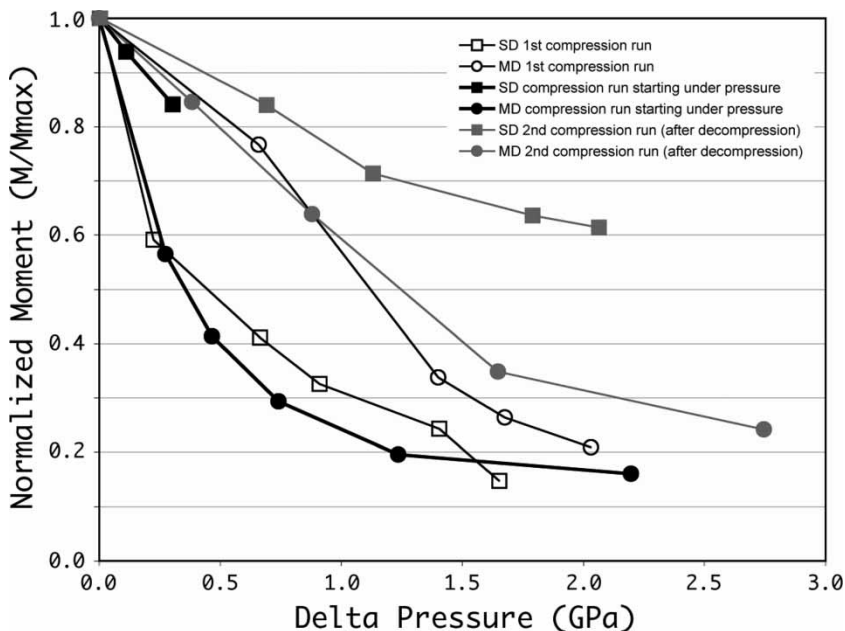


Figure 3. Synthesis of pressure demagnetization results. Single domain (SD) and multidomain (MD) grains originally lying close to the surface will lose half their initial remanence by 0.5 and 1.2 GPa, respectively (open symbols). Grains that formed at depth (filled symbols), then subject to further compression, show nearly the opposite behavior, with MD grains demagnetizing faster than SD grains. For stress-cycled grains, *e.g.*, those previously subjected to stress and then released from stress, then recompressed, multidomain grains show essentially the same behavior as in the initial run, whereas SD magnetite becomes much more resistant (gray symbols). Delta pressure (ΔP) is the pressure at step n (P_n) minus the initial pressure (P_i) when the particular run began ($\Delta P = P_n - P_i$).

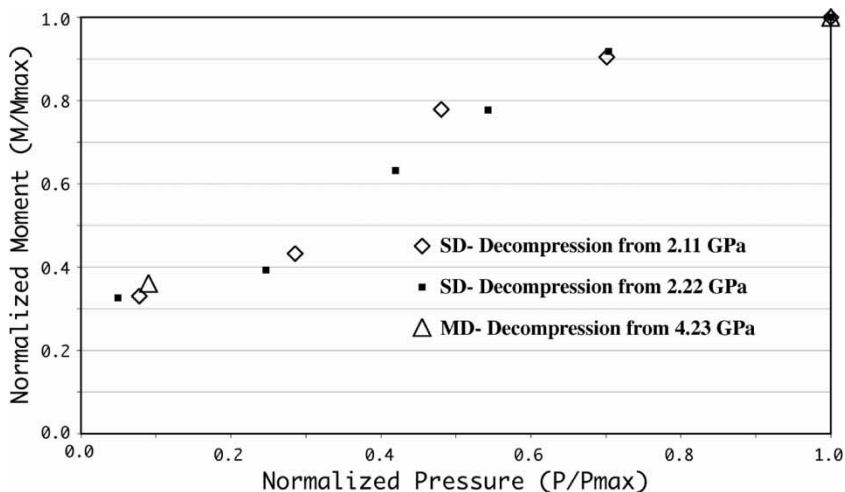


Figure 4. Stress demagnetization of single domain (SD) magnetite under decompression. Two separate runs on the same SD sample yield quite compatible results. Data points at the beginning and end of demagnetization are also shown for multidomain (MD) magnetite. The total relative effect appears to be the same regardless of grain size or starting pressure.

material, although it would be a slight underestimate at higher pressures. We can also propose a specific law that fits each demagnetization curve as

$$M_{P_n}/M_{P_i} = f_{\text{non-demag}} + (1 - f_{\text{non-demag}}) \times \exp(-(P_n/P_c)),$$

where $f_{\text{non-demag}}$ is the fraction of the moment incapable of being demagnetized even at the highest imposed pressures (0.15 seems to best fit the data – figure 3), and P_c is a characteristic pressure parameter which varies from run to run. One varies P_c in order to fit each run; for example, a P_c of 0.4 and 3.0 matches well the first demagnetization run for multidomain magnetite and the third compression run for single domain magnetite, respectively.

The decompression results follow the same trend regardless of the compression path or number of compressions (figure 4). From a maximum initial pressure (P_i), the moment will decrease as $M_{P_n}/M_{P_i} \approx 0.8 \times P_n/P_i + 0.3$ [or $M_{P_n}/M_{P_i} \approx 0.45 \times \ln(P_n/P_i) + 1$, when $P_n > 30\%$ of P_i]. A simplified representation that includes all the decompression data is a law of $M_{P_n}/M_{P_i} = (P_n/P_i)^{0.5}$, with a general rule being that two-thirds of the remanence is lost between the point when compression stops and the end of full decompression ($P_n \approx 0$ GPa). In an absolute sense, demagnetization during pressure release is minor for samples having undergone significant compression (>1 GPa). However, if a rock is exhumed from great depth, as in the central dome region of large craters, decompression demagnetization could be important.

3. Discussion and conclusions

To apply pressure demagnetization in nature, such as on Mars, one needs to know which magnetic phases are being demagnetized. Although pyrrhotite occurs in SNC meteorites, to date only iron oxides (magnetite, maghemite and hematite) have been identified on the Martian surface [32], with magnetite being the only magnetic phase found in igneous outcrops. Moreover, using rock magnetism and thermal modeling, Dunlop and Arkani-Hamed [33] evaluated the candidate minerals responsible for the strong magnetic anomalies of Terra Sirenum and Terra Cimmeria in Mars' southern highlands. The prime candidates, in order of likelihood, are single-domain magnetite, single-domain pyrrhotite and either single or multidomain domain hematite. Thus both direct observation and theoretical considerations suggest magnetite is the most likely magnetic mineral in Martian rocks. If true, then our results confer best with the pressure model of Mohit and Arkani-Hamed [15] for the large Martian craters, as much larger regions should be demagnetized than what is observed when considering other models.

One potential pitfall of our results, as with most of the existing studies [23, 28], is that an isothermal remanent magnetization (IRM), and not a thermal remanent magnetization (TRM), was demagnetized. Assuming that an IRM is more easily demagnetized than a TRM, both our results and the existing ones may be underestimated. On the other hand, shock demagnetization experiments by Pohl *et al.* [25] suggest that samples initially possessing either an IRM or a TRM yield similar results. Our results differ from others in that single domain magnetite demagnetizes faster than multidomain magnetite during the first compression runs. This could be due to the fact that, in our experiments, the dc field was applied perpendicular to the maximum stress direction. As stress reorients Bloch walls [34, 35], and as the reorientation process differs at different pressure intervals [36], the differences are likely linked to the way the domains reorient in relation to the nature of the stress and the angle between the magnetization and applied stress directions. If an IRM is easier to demagnetize than a TRM, the effect is potentially cancelled out by the fact that magnetic moments oriented perpendicular to the maximum stress axis are harder to demagnetize. Another question is whether dynamic

(shock) and static demagnetization are comparable. Shock experiments currently underway suggest this may not be the case for pyrrhotite, but the effects of shock are similar to those found in static experiments on magnetite [37].

With the above-mentioned caveats in mind, our results bear on the way the magnetic signatures of meteorite craters are used to quantify details surrounding impact events. The volume of demagnetized rock, and the level of demagnetization, and the size of the crater, are the key data required to constrain the pressure gradients stemming from the shock [15, 38, 39]. Such knowledge is needed to ascertain the size of the impactor, its impact velocity, impact angle, etc. For the large (300–500 km diameter) Martian meteorite impacts, Mohit and Arkani-Hamed [15] calculated that pressures exceeding 1 GPa extend to about one crater radii away from the center. Other models suggest that the 1 GPa isobar continues significantly farther than two basin radii from the Martian craters [13, 40], and two to four crater radii for the lunar craters [14] (see also refs. [41, 42] for discussion). Another important finding is that, even in the presence of a small (Earth's) magnetic field, both compression and decompression have a demagnetizing effect. These results lead to the important conclusion that one cannot deduce whether a magnetic field existed on a planet based on the magnetic signatures of the rocks in meteorite impact craters at the time of impact.

Acknowledgements

We thank Ales Kapicka and two anonymous reviewers for their helpful suggestions. This is IPGP contribution No. 2171.

References

- [1] T. Nagata and H. Kinoshita, *Nature* **204** 1183 (1964).
- [2] T. Nagata and H. Kinoshita, *J. Geomagn. Geoelectr.* **17** 121 (1965).
- [3] T. Nagata, *J. Geomagn. Geoelectr.* **18** 73 (1966).
- [4] J.P. Pozzi, *Effets de Pression en Magnétisme des Roches*. Ph.D. thesis, Université Paris VI, Paris, France (1973).
- [5] Y. Hamano, *J. Geomagn. Geoelectr.* **35** 155 (1983).
- [6] J.W. Kern, *J. Geophys. Res.* **66** 3807 (1961).
- [7] F.D. Stacey, *Phil. Mag.* **7** 551 (1962).
- [8] F.D. Stacey, *Pure Appl. Geophys.* **58** 5 (1964).
- [9] J. Zlotnicki and F.H. Cornet, *J. Geophys. Res.* **91** 709 (1986).
- [10] B.E. Smith and M.J.S. Johnston, *J. Geophys. Res.* **81**, 3556 (1976).
- [11] M.H. Acuña, J.E.P. Connerney, P. Wasilewski, *et al.*, *J. Geophys. Res.*, E **106** 23403 (2001).
- [12] F. Nimmo and M.S. Gilmore, *J. Geophys. Res. E* **106** 12315 (2001).
- [13] L.L. Hood, N.C. Richmond, E. Pierazzo, *et al.*, *Geophys. Res. Lett.* **30** 1281 doi:10.1029/2002GL016657 (2003).
- [14] J.S. Halekas, D.L. Mitchell, R.P. Lin, *et al.*, *Geophys. Res. Lett.* **29** 1645 doi:10.1029/2001GL013924 (2002).
- [15] P.S. Mohit and J. Arkani-Hamed, *Icarus* **168** 305 (2004).
- [16] D.J. Dunlop, M. Ozima and H. Kinoshita, *J. Geomagn. Geoelectr.* **21** 513 (1969).
- [17] R. Martin and J. Noel, *Geophys. Res. Lett.* **15** 507 (1988).
- [18] K.A. Valeev and S.S. Absalyamov, *Izv. Phys. Solid Earth* **36** 241 (2000).
- [19] W. Kean, R. Day, M. Fuller, *et al.*, *J. Geophys. Res.* **81** 861 (1976).
- [20] M. Lanham and M. Fuller, *Geophys. Res. Lett.* **15** 511 (1988).
- [21] A. Kapicka, *J. Geophys.* **53** 144 (1983).
- [22] A. Kapicka, *Phys. Earth Planet. Int.* **63** 78 (1990).
- [23] G. Kletetschka, J.E.P. Connerney, N.F. Ness, *et al.*, *Meteorit. Planet. Sci.* **39** 1 (2004).
- [24] R.S. Carmichael, *J. Geophys.* **34** 775 (1969).
- [25] J. Pohl, U. Bleil and U. Hornemann, *J. Geophys.* **41** 23 (1975).
- [26] S.M. Cisowski and M. Fuller, *J. Geophys. Res.* **83** 3441 (1978).
- [27] G.J. Borradaile and M. Jackson, *Phys. Earth Planet. Int.* **77** 315 (1993).
- [28] J. Gattacceca, M. Boustie, B.P. Weiss, *et al.*, *Geology* **34** 333 (2006).
- [29] S.A. Gilder, M. Le Goff, J. Peyronneau, *et al.*, *Geophys. Res. Lett.* **29** doi:10.1029/2001GL014227 (2002).
- [30] S.A. Gilder, M. Le Goff, J.-C. Chervin, *et al.*, *Geophys. Res. Lett.* **31** doi:10.1029/2004GL019844 (2004).
- [31] J.C. Chervin, B. Canny and M. Mancinelli, *High Pressure Res.* **21** 305 (2001).
- [32] P. Bertelsen, W. Goetz, M.B. Madsen, *et al.*, *Science* **305** 827 (2004).

- [33] D.J. Dunlop and J. Arkani-Hamed, *J. Geophys. Res.* **110** 1 (2005).
- [34] A.A. Bogdanov and A.Ya. Vlasov, *Izv. Phys. Solid Earth* **1** 24 (1966).
- [35] E. Appel and H.C. Soffel, *Geophys. Res. Lett.* **11** 189 (1984).
- [36] S. Gilder and M. Le Goff, in *Advances in High-Pressure Technology for Geophysical Applications*, edited by J.H. Chen, Y.B. Wang, T.S. Duffy, *et al.* (Elsevier, Amsterdam, 2005), p. 315.
- [37] K.L. Louzada, S.T. Stewart and B.P. Weiss, *Proceedings of the Lunar and Planetary Science Meeting XXXVI* (2005).
- [38] N. Artemieva, L. Hood and B.A. Ivanov, *Geophys. Res. Lett.* **32** L22204 (2005).
- [39] H.A. Ugalde, N. Artemieva and B. Milkereit, *Magnetization on impact structures – Constraints from numerical modeling and petrophysics*, GSA special paper 384: Large Meteorite Impacts III, doi:10.1130/0-8137-2384-1 (2005), p. 25.
- [40] P. Rochette, L. Hood, G. Fillion, *et al.*, *EOS Trans.* **84** 561 (2003).
- [41] P.S. Mohit, *EOS Trans.* **85** 219 (2004).
- [42] P. Rochette, L. Hood, G. Fillion, *et al.*, *EOS Trans.* **85** 219 (2004).